

RESEARCH ARTICLE

UV wing patterns in saturniid moths: diversity and mechanisms

Cédric Finet*, Yuqi Weng, Brian Hanotte* and Antónia Monteiro*

ABSTRACT

Ultraviolet wing patterns are commonly used for intra- and inter-species communication in butterflies. However, as moths have distinct wing resting positions and crepuscular or nocturnal lifestyles, findings in butterflies might not be generalizable to all Lepidoptera. Here, we investigated the location, size and UV reflectance of wing patterns in both sexes of three species of saturniid moths using UV photography. We also investigated the UV reflection mechanisms at the level of individual scales using microspectrophotometry and focused-ion beam scanning electron microscopy. We found that female wings are more UV reflective than male wings and ventral surfaces are more reflective than dorsal surfaces, which is the opposite of what is generally seen in butterflies. The same trend was observed for UV area with an expansion of size in females and ventral wing surfaces. The mechanisms of UV reflection, however, seem to be conserved between saturniid moths and nymphalid butterflies, but not pierids.

KEY WORDS: UV color, Structural coloration, Moths, Wing scales

INTRODUCTION

Animal communication in the ultraviolet (UV) spans a broad range of biological functions. For instance, male lizards use UV throat signals to communicate dominance and to ward off rivals (Fleishman et al., 2011), fiddler crabs use UV signals to select mates (Detto and Backwell, 2009) and yellow damselfish discriminate each other via subtle differences in UV-reflective face patterns (Siebeck et al., 2010). Butterflies also display a range of UV wing patterns that are used both in inter- and intra-specific communication. For example, male *Colias* spp. butterflies use dorsal iridescent UV reflectance in sexual discrimination because females lack this UV signal (Silberglied and Taylor, 1978) and use this male signal in mate assessment (Papke et al., 2007). Both male and female *Heliconius* spp. butterflies use the UV signal in ventral yellow wing bands primarily to recognize and approach conspecifics (Finkbeiner et al., 2017). Female *Bicyclus anynana* rely on the small white reflective eyespot centers, including the UV light, found in male forewings to accept them as mates (Robertson and Monteiro, 2005), whereas males use the same signal on ventral and dorsal surfaces of female forewings to accept them as mates (Prudic et al., 2011; Huq et al., 2019). Female *Eurema hecabe* butterflies prefer males with brighter UV reflectance on most of their dorsal wing surfaces (Kemp, 2008).

UV butterfly wing patterns can be the result of cuticular nano- and microstructures interacting with light, the absence of UV-absorbing

pigments, or a combination of both (recently reviewed in Stella and Kleisner (2022)). In pierids, such as *Colias* spp., the ridges of the wing scales are modified into a series of layered lamellae that act as UV reflectors (Ghiradella et al., 1972; Ghiradella, 1989; Wilts et al., 2011; Ficarrotta et al., 2023) and UV colour saturation is enhanced via pterins that absorb adjacent blue and green wavelengths (Rutowski et al., 2005; Wilts et al., 2011). In *Heliconius* spp., the yellow pigment 3-hydroxy-DL-kynurenine (3-OHK) absorbs light primarily in the blue wavelength range and less in the UV, leaving a minor reflectance band in the UV (Briscoe et al., 2010). In the nymphalid *B. anynana*, the white scales in eyespot centers reflect UV light via scattering (Monteiro et al., 2015), while exhibiting an archetypal structure (Matsuoka and Monteiro, 2018), whereas the silver scales in the same species act as broadband reflectors, including of UV light, via their bilaminar nanostructures with a sandwiched air layer (Ren et al., 2020; Prakash et al., 2022).

The biology of UV wing patterns remains substantially less studied in moths despite being documented by early authors (Mazokhin-Porshniakov, 1957; Eguchi and Meyer-Rochow, 1983). A broad survey of Finnish moths (>700 species) found that 78% of males and females exhibit UV wing patterns (Lyytinen et al., 2004), and a similar approach for moths occurring in the British Isles found that nocturnal species reflect significantly more UV than diurnal (Cane et al., 2018), although these studies did not look into the prevalence of sex-specific, wing-specific or surface-specific distributions of these signals. In the present study, we explore the patterning and the structural basis of the UV reflectance in large population samples of three saturniid moths: the Atlas moth (*Attacus atlas*), the Chinese oak tussar moth (*Antheraea pernyi*) and the Ailanthus silkmoth (*Samia cynthia*). All three species belong to the family Saturniidae, yet they represent different genera, providing phylogenetic breadth within a single, well-defined lineage. These species are also divergent in terms of geography and ecology. The large, short-lived Atlas moth occurs in tropical and subtropical forests in South and Southeast Asia, and inhabits warm, humid and aseasonal niches. The Chinese oak tussar moth, which is semi-domesticated for the production of wild silk, is found in temperate and subtropical deciduous forests in China and East Asia, and faces strong seasonality and often overwinters in diapause. Native to temperate Asia, the Ailanthus silkmoth is now widely distributed and common in urban or disturbed areas; it copes with marked seasonality and is highly adaptable, often thriving near people. The combination of phylogenetic relatedness and contrasting habitat preferences, thermal environments and life-history strategies makes these species an ideal trio to address how environmental and evolutionary pressures shape physiological adaptations such as UV reflection. We applied calibrated UV digital photography, followed by quantification, to characterize and compare the wing UV reflectance within species (between the sexes, fore and hindwings, and dorsal and ventral surfaces) and between species. We then used microspectrophotometry (MSP) and focused-ion beam scanning electron microscopy (SEM) to investigate mechanisms of UV reflection at the level of individual scales.

Biological Sciences, National University of Singapore, Singapore 117543, Singapore.

*Authors for correspondence (cedric.finnet@ens-lyon.org; e0669571@u.nus.edu; antonia.monteiro@nus.edu.sg)

 C.F., 0000-0003-4196-9064; Y.W., 0009-0006-7338-0640; A.M., 0000-0001-9696-459X

Received 18 September 2025; Accepted 19 December 2025

MATERIALS AND METHODS

Biological samples

Specimens of *Antheraea pernyi* (Guérin-Méneville 1855) (15 males, 15 females), *Attacus atlas* (Linnaeus 1758) (16 males, 15 females) and *Samia cynthia* (Drury 1773) (15 males, 15 females), were purchased from the company TimeToBreed (<https://www.timetobreed.com>), a licensed commercial breeder and distributor of both live and dead Lepidoptera. All specimens were newly eclosed of grade A, with no wing damage.

Digital UV photography

Wings isolated from the body were pinned on a Styrofoam support and illuminated with UV light using a 15 W/100 lm UVA bulb (320–400 nm). Images were taken with a Nikon D7100 DSLR camera equipped with a 105 mm *f*/4 UV-Micro-Apo Coastal Optical lens and a Baader U-filter (ZWL 350 nm) (Baader Planetarium). Two diffuse reflectance standards composed of spectralon with a 2% and 99% UV reflectance over the UV-VIS-NIR spectrum (Labsphere, NH, USA) were used for calibration.

Photograph processing

We photographed wings from individual specimens, on dorsal and ventral sides, and processed the photos by largely following the protocol recommended in Napoleone et al. (2022). To identify overexposed or underexposed photos, we used the open-source software RAWTherapee v. 5.1 (<https://rawtherapee.com/>). The ‘neutral’ processing profile was chosen to minimize exposure compensation, which is when the camera automatically adjusts the exposure in challenging lighting conditions.

Photographs were analysed with the open-source software Fiji version 2.30 (Schindelin et al., 2012). The NEF files (Nikon’s RAW file format) were opened with the micaToolbox version 2.2.2 plugin (van den Berg et al., 2020) available from Empirical Imaging (<https://www.empiricalimaging.com/>). While importing the RAW file (Plugins>micaTool>Tools>DCRAW Import), we selected ‘Auto-level brightness’, which keeps the pixel values unaffected and unchecked ‘Camera white balance’, which can produce a higher ratio between the brightest and darkest parts of an image (dynamic range). The photograph’s color channels were split and we kept the green channel, which offered the best contrast.

UV reflectance calculation

Using the polygon selection tool in Fiji, we selected the region of interest (ROI) of the wing, and we measured the mean pixel values within the ROI. We repeated the procedure for both the white and the black standards by moving the same polygon selection tool. For each wing region and standard, we carried out three independent measurements at three non-overlapping locations within the region. Wing region pixel values were compared with those of the white and black standards of known reflectance in the same photograph using the formula:

$$\text{ROI reflectance} = \frac{f - (b_p - c \cdot b_{\%})}{c}, \quad (1)$$

where $c = \frac{w_p - b_p}{w_{\%} - b_{\%}}$, f is the ROI’s measured mean pixel value, b_p is the black standard’s mean pixel value, $b_{\%}$ is the black standard’s percentage reflectance (2%), w_p is the white standard’s mean pixel value and $w_{\%}$ is the white standard’s percentage reflectance (99%).

Percentage area of UV reflectance calculation

Using the freehand selection tool in Fiji, we delineated the entire wing and applied a threshold based on f values for a ROI of 10% (lower threshold level) and 100% (upper threshold level). The areas reflecting at least 10% of UV light were selected and added to the ROI Manager in Fiji using the ‘Analyze particles’ function. The percentage wing area reflecting at least 10% of UV light appeared in the summary table.

Microspectrophotometry

Individual scales were mounted on a glass slide and reflectance spectra were acquired with a microspectrophotometer utilizing a mercury–xenon light source (Thorlabs, NJ, USA) connected to a uSight-2000-Ni microspectrophotometer (Technospec, Singapore), using an Avantes RS-2 mirror tile as a light reference. The microscope’s Nikon TU Plan Fluor objectives 20× (NA=0.5) and 100× (NA=0.9) were used to measure average scale reflectance and ridge or inter-ridge reflectance, respectively. Each measurement was averaged ten times over an integration time of 100 ms. Absorbance spectra were measured using the same setup with the 20× objective, except that the individual scales were mounted on a glass slide, covered with a coverslip, and immersed in clove oil (Hayashi Pure Chemical Ind.), which is a refractive index matching medium for chitin. A transparent area of the covered glass region with clove oil was used as the reference. Both reflectance and absorbance spectra were obtained by averaging three measurements taken at different locations on the same sample. Analysis and spectral plots were done using the R package *pavo 2* (<https://CRAN.R-project.org/package=pavo>; Maia et al., 2019).

Optical imaging

Images of individual scales were recorded using the 20× objective of the same microspectrophotometer setup and a Touptek U3CMOS-05 camera. Scales were individually mounted on a glass slide without a coverslip, and images were taken at different focal planes. Z-stacking was performed using the extended depth of focus function (Process>EDF) in TouptekView software (Touptek). ‘Maximum contrast’ with default settings, followed by ‘no auto Align’, was used as the EDF method.

Scanning electron microscopy and measurements

Samples were mounted on carbon tape and sputter coated (JEOL JFC-1600) with platinum for 30 s at 30 mA. Samples were imaged using a FEI Versa 3D with the following parameters: voltage, 10 kV; current, 23 pA. Cross sections of wing scales were obtained by focused ion beam (FIB) milling using the gallium ion beam of the FEI Versa 3D with the following parameters: beam voltage, 8 kV; beam current, 12 pA; tilt, 52 deg. Scale measurements were taken from SEM images using the line tool implemented in Fiji (Schindelin et al., 2012). Thicknesses were measured from FIB-SEM images using the same tool and corrected for tilted perspective (measured thickness/sin 52 deg) (Villinger et al., 2012). For each scale type, multiple measurements were taken per scale ($n=20$ for the distance ridge–ridge, $n=50$ for the distance crossrib–crossrib, $n=10$ for the lower lamina thickness, $n=10$ for the ridge height) with five scales sampled from one individual.

Statistical analysis

UV reflectance and UV area

We tested whether UV reflectance and UV area were different across sex, wing identity (forewing versus hindwing) and wing surface (dorsal versus ventral). A generalized linear mixed-effects model

(GLMM) was conducted to test how sex, wing identity and wing surface (as main fixed factors) and their interactions impacted UV reflectance or UV area (the dependent factors). Data for the three species were analyzed together with species considered a random factor, i.e. the final models were: UV reflectance (or UV area)~sex*wing identity*wing surface+(1|species). We ran a GLMM using the function `glmer` in the R package *lme4* (<https://CRAN.R-project.org/package=lme4>; Bates et al., 2015). We opted for a gamma distribution which is best for continuous, non-normally distributed data, and we set up the `nAGQ` argument, i.e. the number of points per axis for evaluating the adaptive Gauss–Hermite approximation to the log-likelihood, to 50 which is recommended for small sample sizes. Once the GLMM model was fitted to our data, we ran the model with Type II sums of squares, which is recommended for unbalanced data, using the `Anova` function in the R package *car* (<https://CRAN.R-project.org/package=car>; Fox and Weisberg, 2019). Adjusted *P*-values for different pairwise comparisons were obtained by the Bonferroni *post hoc* test using the R package *emmeans* (<https://CRAN.R-project.org/package=emmeans>; Lenth, 2025). Tukey contrasts were obtained using the R package *multcompView* (<https://CRAN.R-project.org/package=multcompView>). Violin plots were generated using the R package *ggplot2* (<https://cran.r-project.org/src/contrib/Archive/ggplot2/>; Wickham, 2016), and the factor analysis of mixed data (FAMD) plots were generated with the R packages *FactoMineR* (<https://CRAN.R-project.org/package=FactoMineR>; Lê et al., 2008) and *factoextra* (<https://CRAN.R-project.org/package=factoextra>).

Scale morphology

We compared the morphology of UV scales with adjacent non-UV scales within species by measuring mean ridge-ridge distance, crossrib–crossrib distance, lower lamina thickness, and ridge height. Owing to the multilevel context of the datasets, we ran linear mixed-effects (LME) models using the R package *nlme* (<https://CRAN.R-project.org/package=nlme>; Pinheiro et al., 2023), which allows for fixed and random effects. Scale type was treated as the fixed factor and scale replicate nested within individual as a random factor. The lack of homogeneity of variances among scale types prompted us to use the `varIdent` function in the *nlme* package. Akaike information criterion (AIC) was used to compare different models and determine which one was the best for the data. Adjusted *P*-values for multiple pairwise comparisons were obtained by the Bonferroni *post hoc* test with Tukey contrasts using the R package *multcomp* (<https://CRAN.R-project.org/package=multcomp>; Hothorn et al., 2008).

RESULTS

Diversity of UV reflection patterns in Saturniidae

UV reflection was observed in the three species of saturniid moths we investigated. *A. atlas* has qualitatively similar patterns across the sexes (Fig. 1, males; Fig. S1, females), albeit the breadth of the UV reflective regions varies between males and females (Fig. S2). On the dorsal surface, UV light is reflected by the costal margin (forewing and hindwing), the apex (forewing only), ring of marginal eyespot, marginal chevrons, marginal band, discal triangular window, and the proximal and distal white and pink bands of the central symmetry system (CSS) (Figs 1, 2A,B, and Fig. S1). The ventral surfaces exhibit similar UV patterns, but with broader distal bands of the CSS and forewing apices (Fig. 1, Figs S1 and S2).

In male *S. cynthia*, UV light is dorsally reflected by the apex (forewing only), the marginal eyespot ring, anterior marginal band, crescent-shaped transparent discal spots, and the proximal and distal bands of the CSS (Figs 1 and 2A,C). The ventral side showed similar UV patterns but lacked the proximal bands of the CSS

(Fig. 1). Except for the size of some UV reflective regions (Fig. S2), no qualitative difference was observed between *S. cynthia* males and females (Fig. S1).

In male *A. pernyi*, UV light is dorsally reflected by the costal margin (forewing only), a white marginal band stretching into the forewing apex, discal eyespot centers and proximal half of the eyespot outer ring (Figs 1 and 2A,D–F). The ventral sides of the wing exhibit similar UV patterns but have a broader marginal band and more sculpted chevrons along the margin in both forewings and hindwings (Fig. 1 and Fig. S2). UV reflective regions do not substantially differ between *A. pernyi* males and females, except for the ventral hindwing marginal band, which is wider in females (Figs S1 and S2).

UV reflectance

In order to test for differences in UV reflectance between sexes, wing identities (forewing versus hindwing) and wing surfaces (dorsal versus ventral), we averaged the 4–6 most UV reflective regions for each type of wing and compared reflectance across the three saturniid species. We found that UV reflectance differed significantly across the sexes and wing surfaces, as there was also a significant interaction between wing identity and wing surface (Table S1). Wing identity, however, was not a significant predictor of UV reflectance (Table S1).

UV reflectance is sexually dimorphic. When averaged over species, UV reflectance was significantly higher in females compared with males (GLMM, $P<0.0001$) (Fig. S3A and Table S2). Whereas females exhibited significantly higher UV reflectance than males in both *A. atlas* (*post hoc* test from GLMM: adjusted $P<0.0001$) and *A. pernyi* (*post hoc* test from GLMM: adjusted $P<0.0001$) (Fig. 3A and Table S2), UV reflectance was not significantly different between males and females in *S. cynthia* (*post hoc* test from GLMM: adjusted $P=0.15$) (Fig. 3A and Table S2).

We found that UV reflectance did not differ between forewings and hindwings (Fig. 3B, Fig. S3B and Table S2).

Ventral surfaces are more UV-reflective than dorsal surfaces when the three species are analyzed together (GLMM, $P<0.0001$) (Fig. S3C and Table S2). This difference was mostly driven by *A. atlas* (*post hoc* test from GLMM: adjusted $P<0.0001$), whereas the reflectance did not differ between wing sides in *A. pernyi* (*post hoc* test from GLMM: adjusted $P=0.81$) and *S. cynthia* (*post hoc* test from GLMM: adjusted $P=0.99$) (Fig. 3C and Table S2).

UV wing pattern area

In order to test for differences in UV reflective patch area between sexes, wing identities and wing surfaces, we isolated areas that reflected at least 10% of UV light across the different conditions to compare across individuals. We found that sex and wing surface had statistically significant effects on UV reflectance (Table S3). Wing identity, however, was not a significant predictor of UV area (Table S3).

The total UV reflective area was larger in females than in males when the three species were analyzed together (GLMM, $P<0.0001$) (Fig. S4A and Table S4). This was the case for both *A. atlas* (*post hoc* tests from GLMM: adjusted $P<0.0001$) and *A. pernyi* (*post hoc* tests from GLMM: adjusted $P<0.0001$) (Fig. 4A and Table S4). In *S. cynthia*, however, UV area did not differ between male and female wings (*post hoc* tests from GLMM: adjusted $P=0.17$) (Fig. 4A and Table S4). We found that the total UV reflective area did not differ between forewings and hindwings (Fig. 4B, Fig. S4B and Table S4).

The dorsal surface had consistently smaller UV patches than the ventral surface when the three species were analyzed together

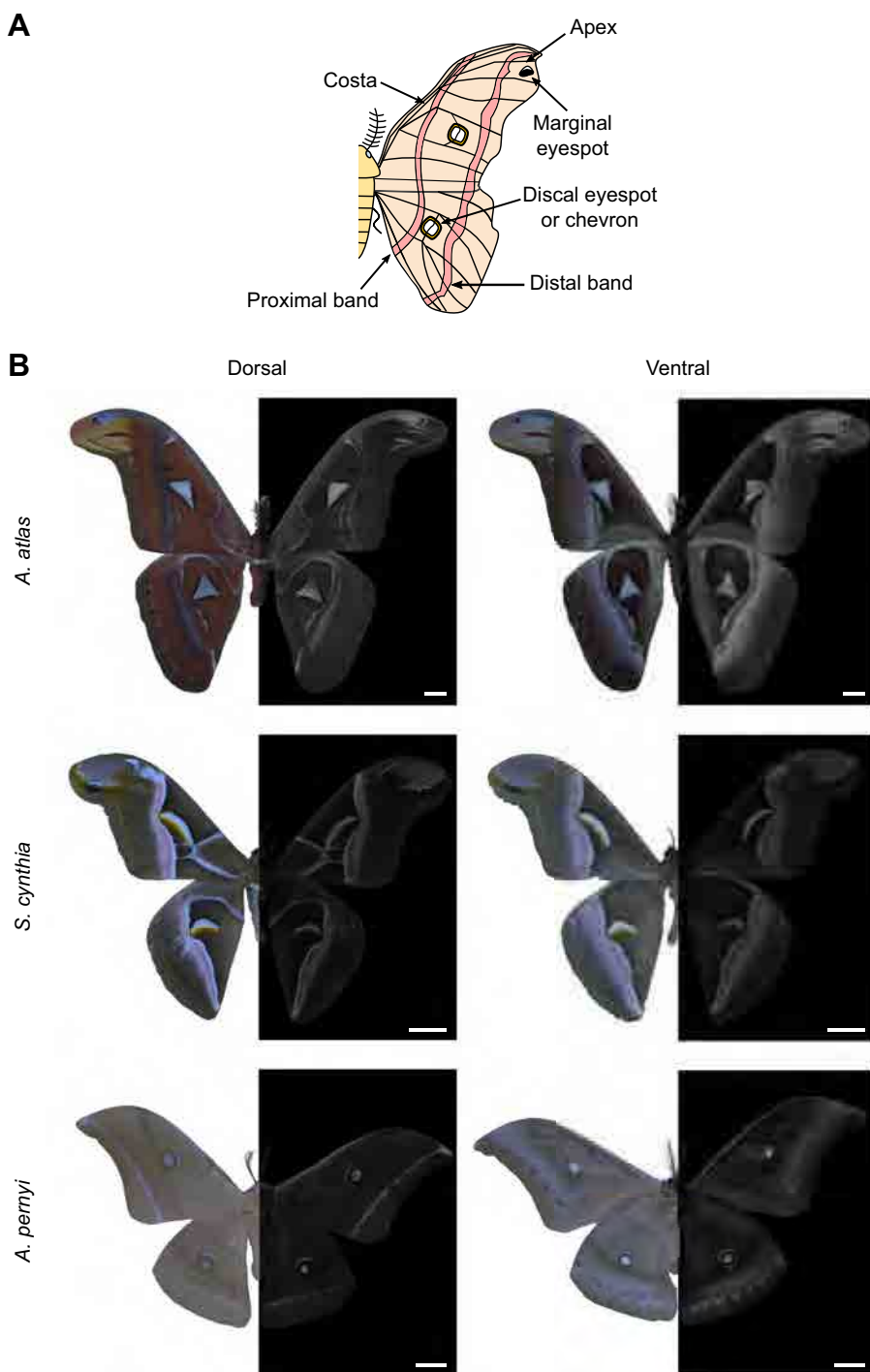


Fig. 1. UV iridescence in three male saturniid species investigated in this study. (A) Moth wing nomenclature used in this study. (B) Each composite panel depicts dorsal and ventral images of the same individual under white light (left half) and UV light (right half, black background). Scale bars: 1 cm.

(GLMM, $P < 0.0001$) (Fig. S4C and Table S4), as well as separately (*post hoc* test from GLMM: adjusted $P < 0.0001$) (Fig. 4C and Table S4).

Optical properties of UV and non-UV reflective scales

We noticed a clear difference in coloration between the UV reflective scales, which were consistently silvery, and the adjacent orange non-UV reflective scales in the apices of all three species (Figs 2B–D, 5A–C, A'–C'), suggesting that low pigmentation may favor UV reflection. In addition, in *A. pernyi* dorsal eyespots, half of the outer ring had white UV reflective scales, whereas the other half had darker non-UV reflective scales (Figs 2E, 5D, D'). In order

to investigate how pigments impacted UV reflectance, we measured the absorbance of individual scales sampled from these locations as a proxy for pigment levels. All UV reflective scales exhibited low pigmentation levels, as measured from very low absorbance (Fig. 5A''–D''). By contrast, non-UV reflective scales absorbed visible light primarily in the wavelength range of 400–550 nm, which is consistent with their orange coloration.

In order to quantify scale reflectance and identify the regions of the scale responsible for the UV signal, we conducted reflectance measurements of individual scales at low and high magnification. At low magnification (20 \times), all UV reflective scales exhibited a reflectance peak in UVA (~ 330 nm) and broadband reflectance

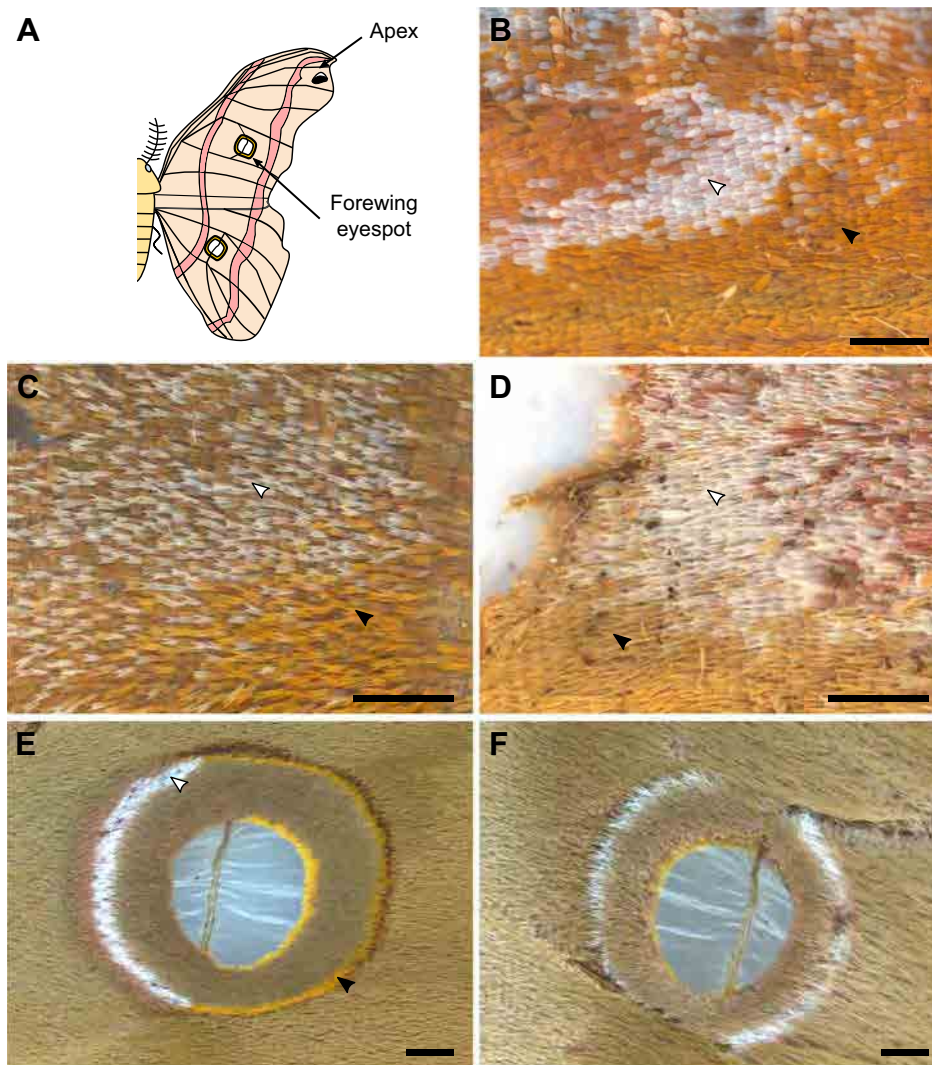


Fig. 2. Magnified views of investigated moth wing areas. (A) The location of the forewing discal eyespot and wing apex and depicted schematically. (B–D) Forewing dorsal apices with white UV reflective scales and orange non-UV reflective scales of (B) *Attacus atlas*, (C) *Samia cynthia* and (D) *Antheraea pernyi*. (E) *A. pernyi* dorsal forewing eyespot with only half of the ring reflecting UV light (white scales on the left). (F) Ventral side of the same wing showing eyespot with the entire white ring reflecting UV light. The location of sampled UV-reflective scales and control scales is indicated with white and black arrowheads, respectively. Scale bars: 1 mm.

between 380 and 700 nm (Fig. S5). All non-UV reflective scales had a similar spectrum, but with a substantial lower intensity in the 330–600 nm wavelength range. This difference in intensity disappeared above 600 nm where both UV and non-UV scales reflected ~7% of the light. At higher magnification (100×), the scale's upper surface appears as a grid of prominent, parallel longitudinal ridges and transverse crossribs that define open windows. We separately measured the light reflected by single ridges and interridge regions centered on the windows. In non-UV reflective scales, these two regions had similar reflectance spectra (Fig. 5A'''–D'''). In UV-reflective scales, the ridges scattered a higher percentage of UV and visible light compared with the interridge region (Fig. 5A'''–D'''), indicating that ridges are especially important for UV reflection.

Fine tuning of geometries in UV reflective scales

Previous studies have shown that the presence of pigments impact the spacings between ridges and crossribs that delineate windows, as well as the upper lamina coverage of those windows (Matsuoka and Monteiro, 2018; Banerjee et al., 2024; Chatterjee et al., 2025 preprint). To test whether similar pigmentation–morphology correlations were present in these moth species, we took SEM images of the scales and measured a series of parameters in UV reflective and pigmented, non-UV reflective scales. We found that

the UV reflective scales with fewer pigments had more covered windows (Fig. 6) and larger distance between ridges (Fig. 7A) and crossribs (Fig. 7B) compared with non-UV reflective scales (ridges: LME, $P < 0.0001$; crossribs: LME, $P < 0.0001$) (Tables S5, S6). On average, UV reflective scales from the wing apex had thinner lower laminae (Fig. 7C) than adjacent non-UV reflective scales (LME, $P < 0.0001$) (Tables S5, S6), but this was not the case for the eyespot ring scales of *A. pernyi* (*post hoc* test from LME: adjusted $P = 1$) (Table S6). On average, UV reflective scales had taller ridges (Fig. 7D) than non-UV reflective scales (LME, $P < 0.0001$) (Tables S5, S6), with the exception of *A. pernyi*, whose UV reflective apical scales had shorter ridges than flanking non-UV reflective scales (*post hoc* test from LME: adjusted $P = 5.22e-13$) (Table S6).

DISCUSSION

UV signals in animals have been primarily associated with reproduction rather than survival advantages, with notable examples in birds (Hunt et al., 1999), fish (Siebeck et al., 2010), reptiles (Fleishman et al., 2011) and arthropods (Detto and Backwell, 2009; Painting et al., 2016; Stella and Kleisner, 2022). In butterflies, UV cues may contribute to species recognition (Silberglied and Taylor, 1973, 1978; Meyer-Rochow, 1991) and sexual selection (Petersen et al., 1951; Brunton and Majerus, 1995; Burghardt et al., 2000; Robertson and Monteiro, 2005; Papke et al., 2007; Kemp, 2008).

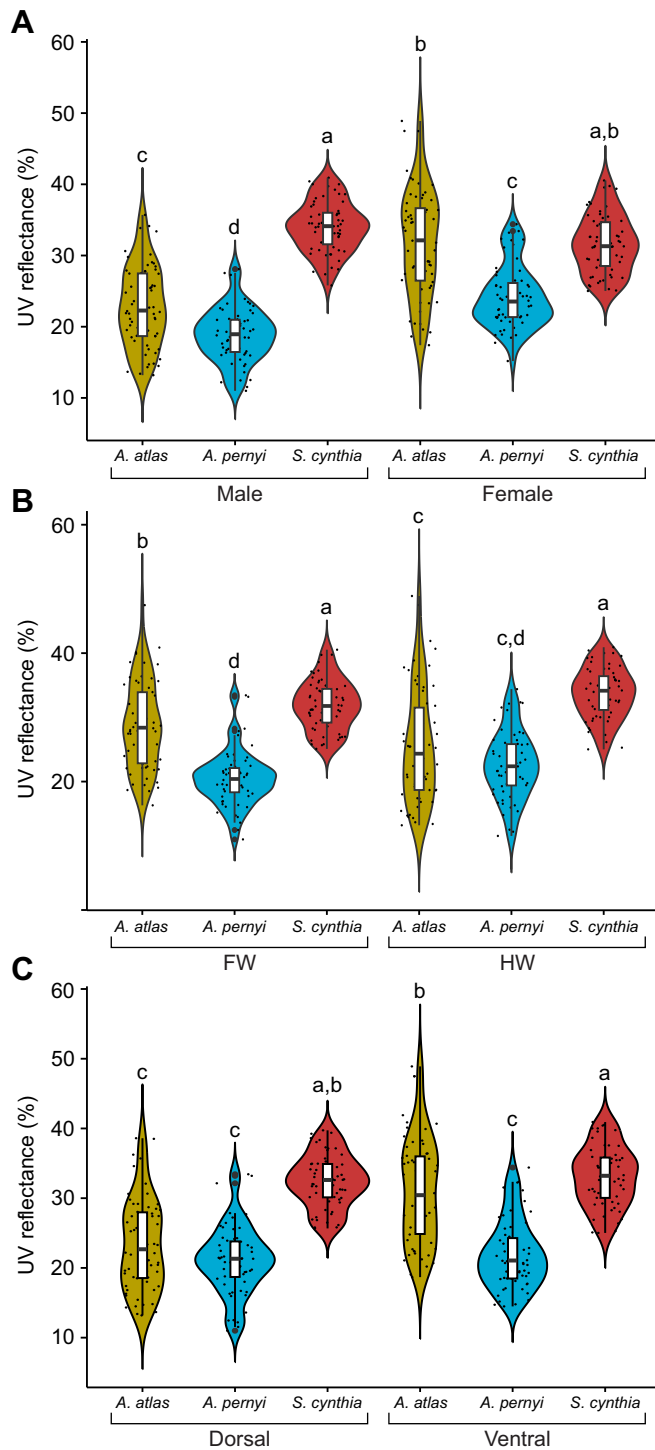


Fig. 3. UV reflectance in the wings of three investigated moth species. UV reflectance across sexes (A), wing identities (B) and wing surfaces (C). The central line in the violin plot indicates the median of the distribution, while the top and bottom of the box represent the third and first quartiles of the data, respectively. Means sharing the same letters are not significantly different (Tukey-adjusted comparisons). The whiskers show up to 1.5 times the inter-quartile range. FW, forewing; HW, hindwing.

However, in rare documented cases, UV coloration can also be linked to crypsis and predator defense functions (Crowell et al., 2024).

The main ecological driver of UV color evolution in moths is still debated but these signals could be involved in sexual signaling. We

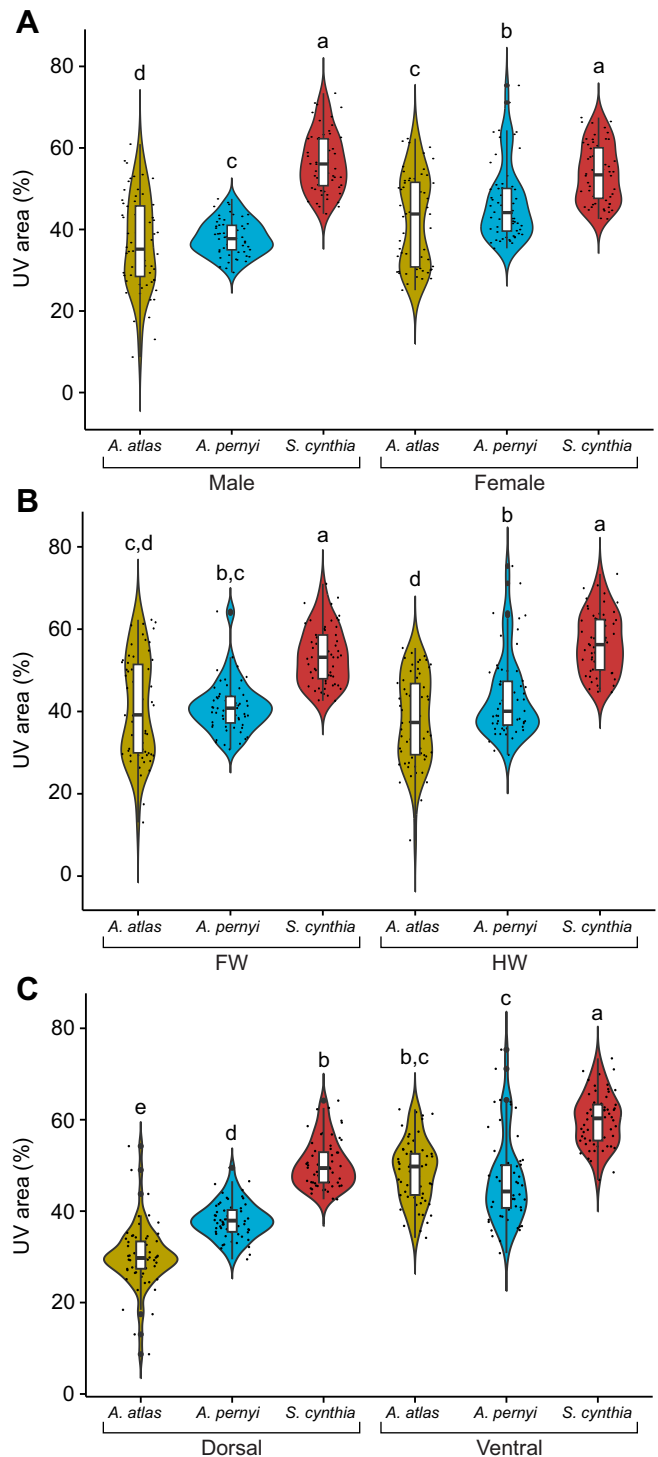


Fig. 4. Percentage of wing area reflecting at least 10% of UV light.

Reflectance across sexes (A), wing identities (B) and wing surfaces (C). The central line in the violin plot indicates the median of the distribution, while the top and bottom of the box represent the third and first quartiles of the data, respectively. Means sharing the same letters are not significantly different (Tukey-adjusted comparisons). The whiskers show up to 1.5 times the inter-quartile range. FW, forewing; HW, hindwing.

found that females of *A. pernyi* and of *A. atlas* had 28% and 40% higher levels, respectively, of UV reflectance than their conspecific males, whereas no sexual dimorphism for this feature was present in *S. cynthia*. In butterflies, males generally signal to females, and it is

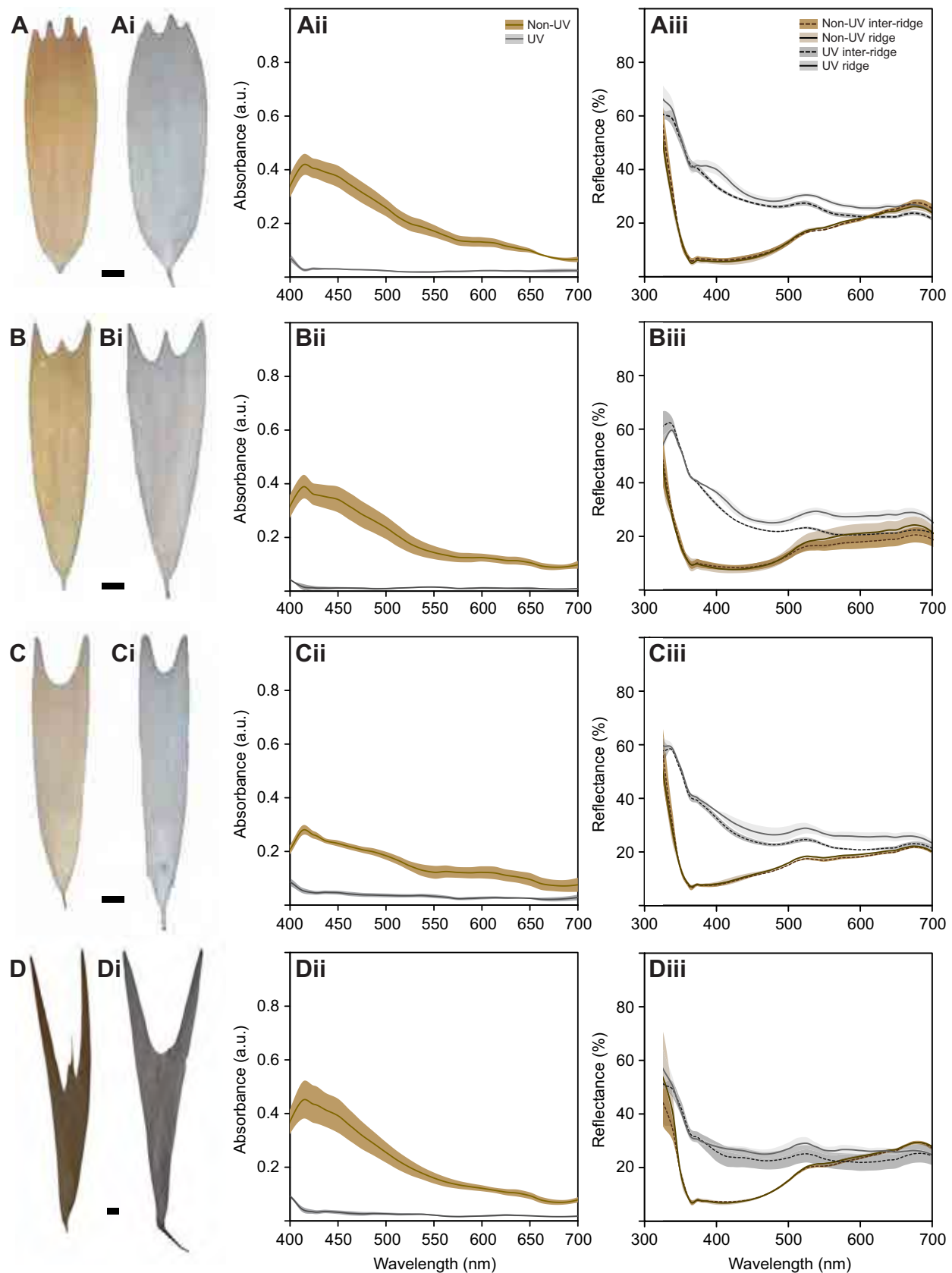


Fig. 5. Optical properties of UV-reflective and adjacent non-UV reflective scales. From left to right: optical microscopy images of the abaxial surfaces of non-UV and UV reflective scales, absorbance spectra and reflectance spectra in *A. atlas* apex (A–Aiii), *S. cynthia* apex (B–Biii), *A. pernyi* apex (C–Ciii) and *A. pernyi* eyespot ring (D–Diii). Scale bars: 20 μm . a.u., arbitrary units.

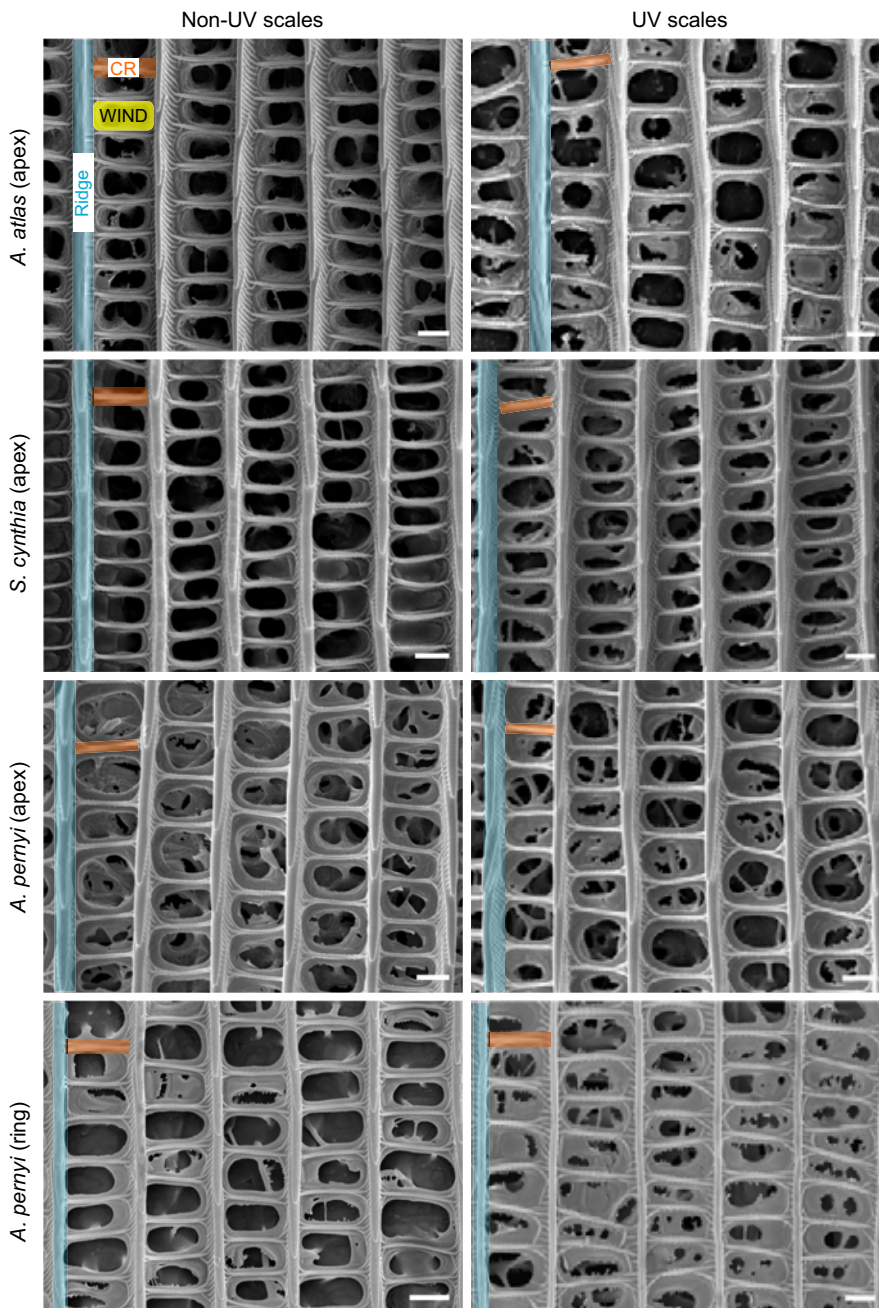


Fig. 6. SEM images of moth wing scales. Non-UV scales have larger windows, with less retained upper lamina, than UV reflective scales. Ridges are highlighted in blue, crossribs (CR) in orange and a window (WIND) is highlighted in yellow. Scale bars: 1 μm.

uncommon for females to exhibit higher UV reflectance levels than males (Mazokhin-Porshniakov, 1957; Wienzek, 1971; Grosman and Stusek, 1982; Eguchi and Meyer-Rochow, 1983; Kemp and Macedonia, 2006). There are, however, a few exceptions known in the Pieridae with a sex role reversal (Stella and Kleisner, 2022). In this family, females of *Pieris napi* display 25–40% higher levels of UV reflectance than males (Meyer-Rochow and Järvillehto, 1997; Stella et al., 2018) and in *P. rapae*, UV reflectance in female wings is crucial for triggering male courtship (Obara, 1970). Male mate preferences, thus, drive this pattern, as previously also proposed for other species (Rutowski et al., 2007; Huq et al., 2019). Therefore, similarly to Pieridae, female saturniid moths may use UV reflectance as a signal during sexual communication, in addition to pheromones (Cardé and Haynes, 2004), and display higher levels of UV in their wings relative to males. In line with this hypothesis, male moths are generally more strongly attracted to UV and blue

light than females are (Garris and Snyder, 2010; Brehm et al., 2021). This is notably the case for *Samia* males as most *Samia* females do not fly towards UV light (Brehm et al., 2021).

Alternatively, sexual differences in UV reflectance may have resulted from natural selection instead of sexual signaling. UV wing patterns seem to be highly attractive to bird predators in the daytime (Viitala et al., 1995; Lyytinen et al., 2001); however, the risk of diurnal predation is probably low for moths whose cryptic wing patterns help in camouflage. More importantly, UV wing patterns do not appear to reduce the fitness of night-active immobilized moths (Lyytinen et al., 2004). Female moths have limited mobility and emit strong pheromones, whereas males are the ones that fly toward the females at night. Natural selection against UV patterns would, thus, be exerted by nocturnal predators relying on UV vision or echolocation. Because males display fewer UV reflective signals and fly at night, we infer that this sex is under stronger selection and under greater risk of predation

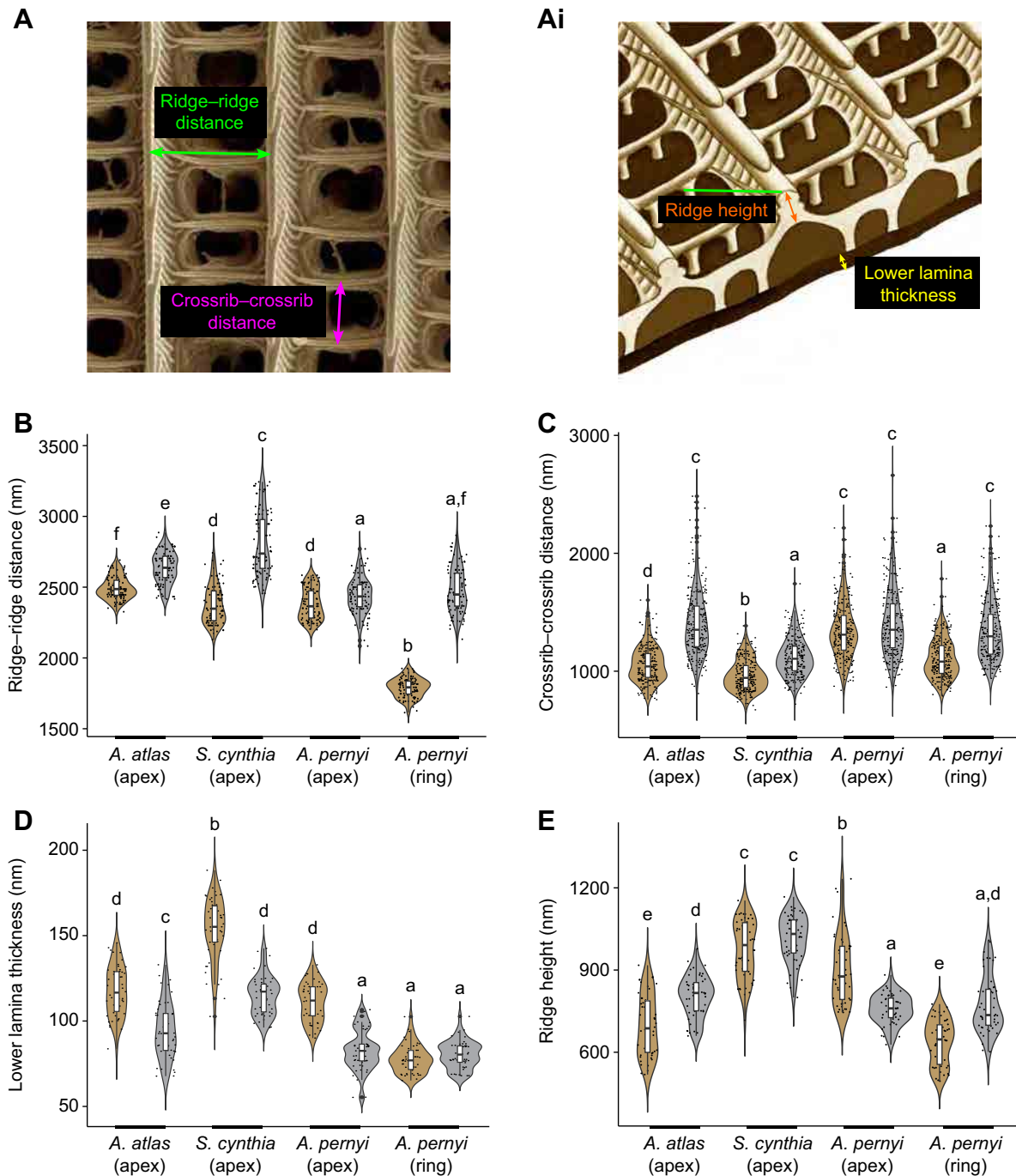


Fig. 7. Characterization of moth wing scale nanomorphology. (A) Top view of a scale illustrating ridge-ridge and crossrib-crossrib distances. (Ai) Cross-section of a scale illustrating lower lamina thickness and ridge height. (B) Distance between two consecutive longitudinal ridges. (C) Distance between two consecutive crossribs. (D) Lower lamina thickness. (E) Ridge height. The central line in the violin plot indicates the median of the distribution, while the top and bottom of the box represent the third and first quartiles of the data, respectively. Means sharing the same letters are not significantly different (Tukey-adjusted comparisons). The whiskers show up to 1.5 times the inter-quartile range.

relative to females. Our findings cannot distinguish which of these two ultimate alternative explanations led to a higher prevalence of UV signals in females, but both may be playing a role in the case of coevolution. Finally, how the angle of incident light may affect the properties of UV reflectance was not examined in this work. However, while angle-dependent reflectance is observed for multilayer reflectors, such as the layered lamellae in pierids (Ghiradella et al., 1972; Wilts et al., 2011), it is less relevant in saturniid moths which have evolved different ways of reflecting UV light.

Signal partitioning between dorsal and ventral wings may be occurring in moths, just as it does in butterflies (Oliver et al., 2009), but our data suggest that the signals are opposite. In butterflies, it is generally accepted that signals on dorsal hidden surfaces of the wing, including UV signals, are used for sexual signaling, whereas colors and patterns on the exposed ventral wing surfaces are used for predator avoidance (Rutowski et al., 2010). Our data for moths show that signal partitioning is also happening, and that the brighter UV signals are found in the hidden wing surfaces. However, in moths,

these are the ventral surfaces. Unlike butterflies, larger moths typically rest with their wings laid flat and/or spread out to their sides, covering the body, with a few exceptions known in the Geometridae. Thus, for the majority of moths, the ventral side of the wing is largely only visible during flight and can be used for private sexual communication.

We have discussed, so far, the reflection spectrum which shows the wavelengths of light that reflect off the wing surface. However, the spectral distribution taken alone does not determine visibility. Diurnal butterflies and crepuscular/nocturnal moths live in different light environments, which impacts their appearance and selective pressure (Sondhi et al., 2021). During the day, sunlight is high in blue and UV radiation, but at night, these levels drop substantially, making nocturnal habitats dark and light limited. Our hypothesis, which posits UV as a communication signal, is supported only if saturniid moths can discriminate color at very low light levels. Notably, saturniids are nocturnal, have superposition eyes optimized for dim light, and have been shown to discriminate colours, including UV, under starlight alone (Anton-Erxleben and Langer, 1988; Warrant and Somanathan, 2022). At the molecular level, our knowledge of the visual system of nocturnal saturniid moths is still scarce. A UV opsin has been identified in *Therinia lactucina* (Sondhi et al., 2021), a short-wavelength/blue opsin in *Saturnia pyri* (Sondhi et al., 2021), and a long-wavelength opsin in *Saturnia pyri* and *Automeris io* (Sondhi et al., 2021; Liénard et al., 2022). Future comparative investigation of opsin expressions in diurnal and nocturnal species of both sexes is essential to complement our understanding of sex-specific coloration in saturniid moths.

To investigate the mechanisms whereby scales become UV reflective in each of the saturniid species, we measured a series of parameters in scales that were previously associated with UV reflectance in butterflies. These included presence/absence of pigments, thickness of the lower lamina, spacing between ridges and cross-ridges, and height of the ridges. UV reflective scales showed consistent low levels of pigmentation as well as consistent morphological modifications that are in line with how structural coloration is produced in stereotypical UV reflective scales of butterflies (Monteiro et al., 2015; Yoda et al., 2021) and also silver scales that act as broadband reflectors (Ren et al., 2020; Prakash et al., 2022). Low pigmentation allows for light to be reflected from the lower lamina to produce structural colors. Interestingly, scales with pigments also had reduced upper cuticular lamina and more open windows. This effect of pigmentation, especially melanin, on creating stronger polymerization of chitin around the ridges and crossribs was previously documented in butterflies (Matsuoka and Monteiro, 2018; Banerjee et al., 2024).

Variation in the thickness of the lower lamina across nymphalid butterflies can change the hue produced by thin-film interference (Stavenga et al., 2014; Wasik et al., 2014; Thayer et al., 2020; Bálint et al., 2023), with the thinnest lower laminae expected to reflect strongly in the UV. Thus, one way to increase UV reflectance is to decrease the thickness of the lower lamina. We observed that in all species investigated, the UV reflective scales had thinner lower laminae than pigmented scales in nearby regions. An exception was seen in the eyespot ring scales in *A. pernyi*, where the pigmented scales (on the distal side of the ring) also had thin lower laminae (~80 nm). Here, the presence and absence of pigments alone was likely contributing to UV reflection differences between the scales on opposite sides of the eyespot.

Increasing the distances between ridges and crossribs is usually understood as a strategy to enhance the light reflected by the lower lamina (Finet et al., 2024 preprint; Banerjee et al., 2024), or the

upper lamina in the case of broadband reflectors (Ren et al., 2020). This wider spacing was observed across all the UV reflective scales sampled here, relative to the pigmented scales. When ridge lamellae are primarily responsible for UV reflectivity, however, dense ridge spacing may evolve instead, as found in some *Heliconius* spp. and *Pieris* spp. butterflies (Kemp et al., 2006; Parnell et al., 2018).

Finally, another strategy to increase UV reflectance is to simply modify the height of the ridges and crossribs, independently of the number and spacing of lamella. The analysis of the direction of the shift in ridge height requires specific attention to the absolute values of this trait in pigmented and UV reflective scales. Our recent related study showed that the same ridge hue, i.e. the wavelength of maximum reflectance, can be achieved for different values of ridge height (Finet et al., 2024 preprint). We conducted our study in stereotypical butterfly scales, but the findings likely stand for all stereotypical scales in Lepidoptera, including moths, because artificial engineered chitosan-based ridges with variable height reproduce the same results (Raut et al., 2022). Thus, ridges are known to reflect UV light when their height is either below 800 nm, in the range 1000–1250 nm or in the range 1500–2000 nm. On average, the ridge height of non-UV reflective apical scales in *S. cynthia* was 976 nm, but UV apical scales in *S. cynthia* have an average height of 1016 nm, the closest morphological solution to become UV reflective. Similarly, UV reflective apical scales in *A. pernyi* evolved shorter ridges (~757 nm), compared with non-UV adjacent scales (~903 nm). In *A. atlas*, both UV reflective and non-reflective scales have ridges that should be mostly UV reflective (~806 and ~696 nm, respectively). Pigments, in this case, have obscured UV reflection in the non-reflective scales.

Conclusion

We found opposite trends in the localization of UV reflection between saturniid moths and butterflies which differ in both wing resting position and lifestyle (nocturnal versus diurnal). UV patterns were more common in the wing surfaces that are hidden, or conditionally displayed, in both groups, which are the ventral surfaces in saturniid moths and dorsal surfaces in butterflies. Given that UV patterns are commonly used in sexual communication in butterflies, we infer that the same happens in saturniid moths. Female saturniids, however, are the sex that exhibited stronger and larger UV-reflective patches, while this pattern is normally seen in male butterflies. These differences between butterflies and saturniid moths suggest that the presence and distribution of UV reflectance across wings and wing surfaces evolved under similar selection pressures in each group but moths may be sex role reversed. Future work could test whether these patterns extend more broadly across moths by examining UV reflectance in non-saturniid lineages (e.g. Geometroidea, Noctuoidea). Additionally, constructing a phylogenetic map of gains and losses of UV reflectance across Lepidoptera would help clarify how many times such patterns have evolved independently and whether similar selective pressures have driven their repeated emergence.

Acknowledgements

We thank Émilie Dion (NUS) and Aswathy Nair (NUS) for helpful discussions on the statistics, Daiqin Li (NUS) for use of the UV camera, Paul Tien Zhi Xian (Lee Kong Chian Natural History Museum) for access to specimens, and the Electron Microscopy Facility (EMF, NUS) for use of FIB-SEM. We also would like to thank Giacomo Viola for his help in the sourcing of high quality saturniid moth specimens.

Competing interests

The authors declare no competing or financial interests.

Author contributions

Conceptualization: C.F., Y.W., B.H., A.M.; Formal analysis: C.F.; Funding acquisition: A.M.; Investigation: Y.W., B.H.; Methodology: C.F., Y.W., B.H.; Resources: B.H.; Supervision: A.M.; Writing – original draft: C.F.; Writing – review & editing: Y.W., B.H., A.M.

Funding

This project was supported by the National Research Foundation Singapore, under the Competitive Research Program award NRF-CRP20-2017-0001, Investigatorship award (NRF-NRFI05-2019-0006) and a Ministry of Education Singapore award (MOE-T2EP30222-0017). B.H. was supported by an NRF Graduate Fellowship.

Data and resource availability

Raw spectral data (absorbance and reflectance), measurements of UV intensities and UV areas, and measurements of scale metrics are downloadable from the public repository Zenodo at doi:10.5281/zenodo.17606467. All other relevant data and details of resources can be found within the article and its supplementary information.

References

- Anton-Erxleben, F. and Langer, H. (1988). Functional morphology of the ommatidia in the compound eye of the moth, *Antheraea polyphemus* (Insecta, Saturniidae). *Cell Tissue Res.* **252**, 385–396. doi:10.1007/BF00214381
- Bálint, Z., Katona, G., Sáfai, S., Collins, S., Piszter, G., Kertész, K. and Biró, L. P. (2023). Measuring and modelling structural colours of *Euphaedra neophron* (Lepidoptera: Nymphalidae) finely tuned by wing scale lower lamina in various subspecies. *Insects* **14**, 303. doi:10.3390/insects14030303
- Banerjee, T. D., Finet, C., Seah, K. S. and Monteiro, A. (2024). Optix regulates nanomorphology of butterfly scales primarily via its effects on pigmentation. *Front. Ecol. Evol.* **12**, 1392050. doi:10.3389/fevo.2024.1392050
- Bates, D., Mächler, M., Bolker, B. M. and Walker, S. C. (2015). Fitting linear mixed-effects models using lme4. *J. Stat. Softw.* **67**, 1–48. doi:10.18637/jss.v067.i01
- Brehm, G., Niermann, J., Jaimes Nino, L. M., Ensling, D., Jüstel, T., Axmacher, J. C., Warrant, E. and Fiedler, K. (2021). Moths are strongly attracted to ultraviolet and blue radiation. *Insect Conserv. Divers.* **14**, 188–198. doi:10.1111/icad.12476
- Briscoe, A. D., Bybee, S. M., Bernard, G. D., Yuan, F., Sison-Mangus, M. P., Reed, R. D., Warren, A. D., Llorente-Bousquets, J. and Chiao, C. C. (2010). Positive selection of a duplicated UV-sensitive visual pigment coincides with wing pigment evolution in *Heliconius* butterflies. *Proc. Natl. Acad. Sci. USA* **107**, 3628–3633. doi:10.1073/pnas.0910085107
- Brunton, C. F. A. and Majerus, M. E. N. (1995). Ultraviolet colours in butterflies: intra- or inter-specific communication? *Proc. R. Soc. B Biol. Sci.* **260**, 199–204. doi:10.1098/rspb.1995.0080
- Burghardt, F., Knüttel, H., Becker, M. and Fiedler, K. (2000). Flavonoid wing pigments increase attractiveness of female common blue (*Polyommatus icarus*) butterflies to mate-searching males. *Naturwissenschaften* **87**, 304–307. doi:10.1007/s001140050726
- Cane, E., Laventhol, J. and Ledger, S. (2018). Surveying ultraviolet reflectance in moths: a method and workflow for data capture using open-source tools. *J. Nat. Sci. Collect.* **5**, 50–65.
- Cardé, R. and Haynes, K. (2004). Structure of the pheromone communication channel in moths. In *Advances in Insect Chemical Ecology* (ed. R. Cardé and J. Millar), pp. 283–332. Cambridge: Cambridge University Press.
- Chatterjee, M., Finet, C., Siegel, K. J., Loh, L. S., Delgado, S., McDonald, J. M. C., Markenscoff-Papadimitriou, E., Monteiro, A. and Reed, R. D. (2025). Butterfly wing iridescence is regulated by araucan, a direct target of optix and spalt. *bioRxiv*. doi:10.1101/2023.11.21.568172
- Crowell, H., Curlis, J., Weller, H. and Rabosky, A. (2024). Ecological drivers of ultraviolet colour evolution in snakes. *Nat. Commun.* **15**, 5213. doi:10.1038/s41467-024-49506-4
- Detto, T. and Backwell, P. R. Y. (2009). The fiddler crab *Uca mjoebergi* uses ultraviolet cues in mate choice but not aggressive interactions. *Anim. Behav.* **78**, 407–411. doi:10.1016/j.anbehav.2009.05.014
- Eguchi, E. and Meyer-Rochow, B. (1983). Ultraviolet photography of forty-three species of Lepidoptera representing ten families. *Annot. Zool. Jpn.* **56**, 10–18.
- Ficarrotta, V., Martin, A., Counterman, B. A. and Alexander Pyron, R. (2023). Early origin and diverse phenotypic implementation of iridescent UV patterns for sexual signaling in pierid butterflies. *Evolution (N. Y.)* **77**, 2619–2630. doi:10.1093/evolut/qpad174
- Finet, C., Ruan, Q., Bei, Y. Y., Saranathan, V. and Monteiro, A. (2024). Ridge and crossrib height of butterfly wing scales is a toolbox for structural color diversity. *bioRxiv*. doi:10.1101/2024.03.28.585318
- Finkbeiner, S. D., Fishman, D. A., Osorio, D. and Briscoe, A. D. (2017). Ultraviolet and yellow reflectance but not fluorescence is important for visual discrimination of conspecifics by *Heliconius erato*. *J. Exp. Biol.* **220**, 1267–1276. doi:10.1242/jeb.153593
- Fleishman, L. J., Loew, E. R. and Whiting, M. J. (2011). High sensitivity to short wavelengths in a lizard and implications for understanding the evolution of visual systems in lizards. *Proc. R. Soc. B Biol. Sci.* **278**, 2891–2899. doi:10.1098/rspb.2011.0118
- Fox, J. and Weisberg, S. (2019). *An R Companion to Applied Regression*, 3rd edn. Sage.
- Garris, H. W. and Snyder, J. A. (2010). Sex-specific attraction of moth species to ultraviolet light traps. *Southeast. Nat.* **9**, 427–434. doi:10.1656/058.009.0302
- Ghiradella, H. (1989). Structure and development of iridescent butterfly scales: lattices and laminae. *J. Morphol.* **202**, 69–88. doi:10.1002/jmor.1052020106
- Ghiradella, H., Aneshansley, D., Eisner, T., Silberglied, R. E. and Hinton, H. E. (1972). Ultraviolet reflection of a male butterfly: interference color caused by thin-layer elaboration of wing scales. *Science* **178**, 1214–1217. doi:10.1126/science.178.4066.1214
- Grosman, M. and Stusek, P. (1982). Parametri odbite svetlobe s kril metuljev. *Biol. Vestn.* **30**, 59–84.
- Hothorn, T., Bretz, F. and Westfall, P. (2008). Simultaneous inference in general parametric models. *Biom. J.* **50**, 346–363. doi:10.1002/bimj.200810425
- Hunt, S., Cuthill, I. C., Bennett, A. T. D. and Griffiths, R. (1999). Preferences for ultraviolet partners in the blue tit. *Anim. Behav.* **58**, 809–815. doi:10.1006/anbe.1999.1214
- Huq, M., Bhardwaj, S. and Monteiro, A. (2019). Male *Bicyclus anynana* butterflies choose females on the basis of their ventral UV-reflective eyespot centers. *J. Insect Sci.* **19**, 1–8. doi:10.1093/jisesa/iez014
- Kemp, D. J. (2008). Female mating biases for bright ultraviolet iridescence in the butterfly *Eurema hecabe* (Pieridae). *Behav. Ecol.* **19**, 1–8. doi:10.1093/beheco/arm094
- Kemp, D. J. and Macedonia, J. M. (2006). Structural ultraviolet ornamentation in the butterfly *Hypolimnas bolina* L. (Nymphalidae): visual, morphological and ecological properties. *Aust. J. Zool.* **54**, 235–244. doi:10.1071/ZO06005
- Kemp, D. J., Vukusic, P. and Rutowski, R. L. (2006). Stress-mediated covariance between nano-structural architecture and ultraviolet butterfly coloration. *Funct. Ecol.* **20**, 282–289. doi:10.1111/j.1365-2435.2006.01100.x
- Lê, S., Josse, J. and Husson, F. (2008). FactoMineR: an R package for multivariate analysis. *J. Stat. Softw.* **25**, 1–18. doi:10.18637/jss.v025.i01
- Liénard, M. A., Valencia-Montoya, W. A. and Pierce, N. E. (2022). Molecular advances to study the function, evolution and spectral tuning of arthropod visual opsins. *Philos. Trans. R. Soc. B Biol. Sci.* **377**, 20210279. doi:10.1098/rstb.2021.0279
- Lyytinen, A., Alatalo, R. V., Lindström, L. and Mappes, J. (2001). Can ultraviolet cues functions as aposematic signals? *Behav. Ecol.* **12**, 65–70. doi:10.1093/oxfordjournals.beheco.a000380
- Lyytinen, A., Lindström, L. and Mappes, J. (2004). Ultraviolet reflection and predation risk in diurnal and nocturnal Lepidoptera. *Behav. Ecol.* **15**, 982–987. doi:10.1093/beheco/arl102
- Maia, R., Gruson, H., Endler, J. A. and White, T. E. (2019). pavo 2: new tools for the spectral and spatial analysis of colour in R. *Methods Ecol. Evol.* **10**, 1097–1107. doi:10.1111/2041-210X.13174
- Matsuoka, Y. and Monteiro, A. (2018). Melanin pathway genes regulate color and morphology of butterfly wing scales. *Cell Rep.* **24**, 56–65. doi:10.1016/j.celrep.2018.05.092
- Mazokhin-Porshniakov, G. A. (1957). Reflecting properties of butterfly wings and role of ultra-violet rays in the vision of insects. *Biofizika* **2**, 358–368.
- Meyer-Rochow, V. B. (1991). Differences in ultraviolet wing patterns in the New Zealand lycaenid butterflies *Lycaena salustius*, *L. rauparaha*, and *L. feredayi* as a likely isolating mechanism. *J. R. Soc. N. Z.* **21**, 169–177. doi:10.1080/03036758.1991.10431405
- Meyer-Rochow, V. B. and Järvielto, M. (1997). Ultraviolet colours in *Pieris napi* from northern and southern Finland: arctic females are the brightest!. *Naturwissenschaften* **84**, 165–168. doi:10.1007/s001140050373
- Monteiro, A., Tong, X., Bear, A., Liew, S. F., Bhardwaj, S., Wasik, B. R., Dinwiddie, A., Bastianelli, C., Cheong, W. F., Wenk, M. R. et al. (2015). Differential expression of ecdysone receptor leads to variation in phenotypic plasticity across serial homologs. *PLoS Genet.* **11**, e1005529. doi:10.1371/journal.pgen.1005529
- Napoleone, F., Manzini, D. and Burrascano, S. (2022). How to measure flower ultraviolet reflectance using digital photography. *Appl. Veg. Sci.* **25**, e12648. doi:10.1111/avsc.12648
- Obara, Y. (1970). Studies on the mating behavior of the white cabbage butterfly, *Pieris rapae crucivora* Boisduval - III. Near-ultra-violet reflection as the signal of intraspecific communication. *Z. Vgl. Physiol.* **69**, 99–116. doi:10.1007/BF00340912
- Oliver, J. C., Robertson, K. A. and Monteiro, A. (2009). Accommodating natural and sexual selection in butterfly wing pattern evolution. *Proc. R. Soc. B Biol. Sci.* **276**, 2369–2375. doi:10.1098/rspb.2009.0182
- Painting, C. J., Rajamohan, G., Chen, Z., Zeng, H. and Li, D. (2016). It takes two peaks to tango: the importance of UVB and UVA in sexual signalling in jumping spiders. *Anim. Behav.* **113**, 137–146. doi:10.1016/j.anbehav.2015.12.030
- Papke, R. S., Kemp, D. J. and Rutowski, R. L. (2007). Multimodal signalling: structural ultraviolet reflectance predicts male mating success better than

- pheromones in the butterfly *Colias eurytheme* L. (Pieridae). *Anim. Behav.* **73**, 47–54. doi:10.1016/j.anbehav.2006.07.004
- Parnell, A. J., Bradford, J. E., Curran, E. V., Washington, A. L., Adams, G., Brien, M. N., Burg, S. L., Morochz, C., Fairclough, J. P. A., Vukusic, P. et al. (2018). Wing scale ultrastructure underlying convergent and divergent iridescent colours in mimetic *Heliconius* butterflies. *J. R. Soc. Interface* **15**, 20170948. doi:10.1098/rsif.2017.0948
- Petersen, B., Törnblom, O. and Bodin, N.-O. (1951). Verhaltensstudien Am Rapsweissling Und Bergweissling (Pieris Napi L. und Pieris Bryoniae Ochs.). *Behaviour* **4**, 67–84. doi:10.1163/156853951X00043
- Prakash, A., Finet, C., Banerjee, T. D., Saranathan, V. and Monteiro, A. (2022). Antennapedia and optix regulate metallic silver wing scale development and cell shape in *Bicyclus anynana* butterflies. *Cell Rep.* **40**, 111052. doi:10.1016/j.celrep.2022.111052
- Prudic, K. L., Jeon, C., Cao, H. and Monteiro, A. (2011). Developmental plasticity in sexual roles of butterfly species drives mutual sexual ornamentation. *Science* **331**, 73–75. doi:10.1126/science.1197114
- Raut, H. K., Ruan, Q., Finet, C., Saranathan, V., Yang, J. K. W. and Fernandez, J. G. (2022). The height of chitinous ridges alone produces the entire structural color palette. *Adv. Mater. Interfaces* **9**, 2201419. doi:10.1002/admi.202201419
- Ren, A., Day, C. R., Hanly, J. J., Counterman, B. A., Morehouse, N. I. and Martin, A. (2020). Convergent evolution of broadband reflectors underlies metallic coloration in butterflies. *Front. Ecol. Evol.* **8**, 206. doi:10.3389/fevo.2020.00206
- Robertson, K. A. and Monteiro, A. (2005). Female *Bicyclus anynana* butterflies choose males on the basis of their dorsal UV-reflective eyespot pupils. *Proc. R. Soc. B Biol. Sci.* **272**, 1541–1546. doi:10.1098/rspb.2005.3142
- Rutowski, R. L., Macedonia, J. M., Morehouse, N. and Taylor-Taft, L. (2005). Pterin pigments amplify iridescent ultraviolet signal in males of the orange sulphur butterfly, *Colias eurytheme*. *Proc. R. Soc. B Biol. Sci.* **272**, 2329–2335. doi:10.1098/rspb.2005.3216
- Rutowski, R. L., Macedonia, J. M., Kemp, D. J. and Taylor-Taft, L. (2007). Diversity in structural ultraviolet coloration among female sulphur butterflies (Coliadinae, Pieridae). *Arthropod Struct. Dev.* **36**, 280–290. doi:10.1016/j.asd.2006.11.005
- Rutowski, R. L., Nahm, A. C. and Macedonia, J. M. (2010). Iridescent hindwing patches in the pipevine swallowtail: differences in dorsal and ventral surfaces relate to signal function and context. *Funct. Ecol.* **24**, 767–775. doi:10.1111/j.1365-2435.2010.01693.x
- Schindelin, J., Arganda-Carreras, I., Frise, E., Kaynig, V., Longair, M., Pietzsch, T., Preibisch, S., Rueden, C., Saalfeld, S., Schmid, B. et al. (2012). Fiji: an open-source platform for biological-image analysis. *Nat. Methods* **9**, 676–682. doi:10.1038/nmeth.2019
- Siebeck, U. E., Parker, A. N., Sprenger, D., Mähger, L. M. and Wallis, G. (2010). A species of reef fish that uses ultraviolet patterns for covert face recognition. *Curr. Biol.* **20**, 407–410. doi:10.1016/j.cub.2009.12.047
- Silberglied, R. E. and Taylor, O. R. (1973). Ultraviolet differences between the sulphur butterflies, *Colias eurytheme* and *C. philodice*, and a possible isolating mechanism. *Nature* **241**, 406–408. doi:10.1038/241406a0
- Silberglied, R. E. and Taylor, O. R. (1978). Ultraviolet reflection and its behavioral role in the courtship of the sulfur butterflies *Colias eurytheme* and *C. philodice* (Lepidoptera, Pieridae). *Behav. Ecol. Sociobiol.* **3**, 203–243. doi:10.1007/BF00296311
- Sondhi, Y., Ellis, E. A., Bybee, S. M., Theobald, J. C. and Kawahara, A. Y. (2021). Light environment drives evolution of color vision genes in butterflies and moths. *Commun. Biol.* **4**, 177. doi:10.1038/s42003-021-01688-z
- Stavenga, D. G., Leertouwer, H. L. and Wilts, B. D. (2014). Coloration principles of nymphaline butterflies - Thin films, melanin, ommochromes and wing scale stacking. *J. Exp. Biol.* **217**, 2171–2180. doi:10.1242/jeb.098673
- Stella, D. and Kleisner, K. (2022). Visible beyond violet: how butterflies manage ultraviolet. *Insects* **13**, 242. doi:10.3390/insects13030242
- Stella, D., Pecháček, P., Meyer-Rochow, V. B. and Kleisner, K. (2018). UV reflectance is associated with environmental conditions in palaeartic *Pieris napi* (Lepidoptera: Pieridae). *Insect Sci.* **25**, 508–518. doi:10.1111/1744-7917.12429
- Thayer, R., Allen, F. and Patel, N. H. (2020). Structural color in Junonia butterflies evolves by tuning scale lamina thickness. *eLife* **9**, e52187. doi:10.7554/eLife.52187
- van den Berg, C. P., Troscianko, J., Endler, J. A., Marshall, N. J. and Cheney, K. L. (2020). Quantitative Colour Pattern Analysis (QCPA): a comprehensive framework for the analysis of colour patterns in nature. *Methods Ecol. Evol.* **11**, 316–332. doi:10.1111/2041-210X.13328
- Viitala, J., Korpimäki, E., Palokangas, P. and Koivula, M. (1995). Attraction of kestrels to vole scent marks visible in ultraviolet light. *Nature* **373**, 425–427. doi:10.1038/373425a0
- Villinger, C., Gregorius, H., Kranz, C., Höhn, K., Münzberg, C., Von Wichert, G., Mizaikoff, B., Wanner, G. and Walther, P. (2012). FIB/SEM tomography with TEM-like resolution for 3D imaging of high-pressure frozen cells. *Histochem. Cell Biol.* **138**, 549–556. doi:10.1007/s00418-012-1020-6
- Warrant, E. and Somanathan, H. (2022). Colour vision in nocturnal insects. *Philos. Trans. R. Soc. B Biol. Sci.* **377**, 20210285. doi:10.1098/rstb.2021.0285
- Wasik, B. R., Liew, S. F., Lilien, D. A., Dinwiddie, A. J., Noh, H., Cao, H. and Monteiro, A. (2014). Artificial selection for structural color on butterfly wings and comparison with natural evolution. *Proc. Natl. Acad. Sci. USA* **111**, 12109–12114. doi:10.1073/pnas.1402770111
- Wickham, H. (2016). *ggplot2: Elegant Graphics for Data Analysis*. New York: Springer-Verlag.
- Wienzek, M. (1971). Spektrale Reflektionsmessungen an Insektenintegumenten. *Forma Funct.* **4**, 340–381.
- Wilts, B. D., Pirih, P. and Stavenga, D. G. (2011). Spectral reflectance properties of iridescent pierid butterfly wings. *J. Comp. Physiol. A Neuroethol. Sensory Neural Behav. Physiol.* **197**, 673–702. doi:10.1007/s00359-011-0632-y
- Yoda, S., Sakakura, K., Kitamura, T., KonDo, Y., Sato, K., Ohnuki, R., Someya, I., Komata, S., Kojima, T., Yoshioka, S. et al. (2021). Genetic switch in UV response of mimicry-related pale-yellow colors in Batesian mimic butterfly, *Papilio polytes*. *Sci. Adv.* **7**, eabd6475. doi:10.1126/sciadv.abd6475